

# Pion structure in Holographic QCD

Jiali Deng\* and Defu Hou

*Institute of Particle Physics and Key Laboratory of Quark and Lepton Physics (MOS),  
Central China Normal University, Wuhan 430079, China*

(Dated: June 5, 2026)

We employ a holographic model with a modified background that incorporates effective descriptions of key QCD features, including linear confinement and gluon condensation, to study the pion's internal structure, encompassing its mass spectrum as well as electromagnetic and gravitational form factors. This model is capable of simultaneously describing these diverse observables and reaches reasonable agreement with both experimental measurements and lattice QCD results. Our findings indicate that the model captures essential aspects of the pion. The description of multiple structure observables supports its potential as a useful tool for further investigations of pion properties.

## I. INTRODUCTION

As the simplest quark-antiquark bound state and a Nambu-Goldstone boson of spontaneous chiral symmetry breaking, the pion is crucially linked to both strong force and the origin of hadronic mass, playing a pivotal role in QCD (see, e.g., Refs. [1–3]). Paradoxically, despite being theoretically simpler than the proton, its internal structure remains less well understood [4].

A particularly relevant class of models are those based on the anti-de Sitter/conformal field theory (AdS/CFT) correspondence [5–7]. The breaking of conformal invariance yields effective theories known as holographic QCD or AdS/QCD models. The hard wall model breaks conformal symmetry by introducing a hard cutoff in the holographic coordinate, and the soft wall model is implemented by introducing a soft cutoff via a dilaton field in the action [8–10]. Alternative methods include modifying the warp factor within the  $AdS_5$  metric [11–14]. These models have successfully addressed many problems in QCD's strongly coupled regime. A key advantage is their ability to incorporate both small and large momentum transfer regimes without an inherent limit on  $Q^2$ . This stands in contrast to experiments and other approaches like QCD Sum Rules [15, 16], which typically are confined to specific momentum transfer windows. This makes the AdS/QCD framework a particularly effective tool for exploring non-perturbative hadron properties beyond the reach of perturbative methods.

These approaches have enabled significant progress on key pion properties. The mass spectrum—a foundational benchmark—has been investigated holographically and by other frameworks, establishing a calibration baseline [17–21]. Complementing this, the electromagnetic form factors (EMFF) of the pion, which encode its charge distribution, have been investigated via pion electroproduction experiments and through theoretical approaches such as holographic QCD and lattice QCD [22–29]. Similarly, the gravitational form factors (GFFs) of the pion, which reveal its mass and force distributions, remain the subject of active study. Primarily accessed through

theoretical tools such as holographic QCD and lattice QCD [30–36], they also motivate experimental searches in channels like exclusive meson photoproduction [37].

Despite significant progress, certain limitations persist. Current holographic studies of the pion's internal structure typically examine its mass spectrum, EMFF, and GFF separately, relying on different parameter sets or distinct models for each. A comprehensive holographic calculation, capable of simultaneously reproducing the pion's mass spectrum while predicting its EMFF, radii and GFF, has not been fully achieved—which is essential for validating a model's robustness and ensuring a single parameterization describes a wide array of pion properties

In this work, we explore a possible way to approach these problems by modifying the warp factors in the  $AdS_5$  metric, rather than introducing a dilaton field in the action. We employ this modified holographic model, which incorporates essential QCD features such as linear confinement and gluon condensation, to investigate the pion's internal structure. We begin by computing the pion's mass spectrum to determine the model parameters. Then, using this set of parameters, we predict the pion's electromagnetic form factors (including the charge radius) and gravitational form factors, and compare them with experimental data and lattice results. The calculated pion structure shows consistency with experimental data and lattice results. Finally, we extend the calculation to explore the dependence of form factors on the pion mass and compute them for pion excited states.

The remainder of the paper is structured as follows: We begin by introducing the soft-wall holographic QCD framework and detailing the pion mass spectrum calculation in Section II. We then predict the pion's electromagnetic form factor in Section III, and derive and analyze the gravitational form factor in Section IV. Next, we extend the calculation to explore the mass dependence of the form factors and compute those for pion excited states in Section V. Finally, Section VI summarizes and discusses the broader implications of our key findings.

---

\* dj12022010355@mails.ccnu.edu.cn, houdf@mail.ccnu.edu.cn

## II. MASS SPECTRUM FOR PION

In this section, we introduce a phenomenologically corrected holographic model and use it to calculate the mass spectrum of pion mesons. The holographic soft-wall model is the most widely used approach, partly because the soft cutoff it introduces is more natural than the hard cutoff of the hard-wall model, and partly because it can generate linear Regge behavior. In the original soft-wall model, The spacetime metric is given by [10]

$$ds^2 = \frac{1}{z^2}(\eta_{\mu\nu}dx^\mu dx^\nu + dz^2), \quad (1)$$

where  $\eta_{\mu\nu}$  denotes the four-dimensional Minkowski metric tensor with signature  $(-, +, +, +)$  and  $z$  is the holographic coordinate in the fifth dimension, with the boundary at  $z = 0$  corresponding to the ultraviolet (UV) regime of the dual field theory. The action can be expressed as:

$$S = \int d^4x dz \sqrt{-g} e^{-\lambda_0(z)} \ell, \quad (2)$$

where  $\lambda_0(z) = c_0^2 z^2$  represents the dilaton field, with  $c_0$  a free parameter, and  $\ell$  denotes the Lagrangian density. This action can reproduce the confinement properties of QCD. To construct a model that more closely approximates real QCD, an alternative form of the dilaton field can be expressed as [38–40]:

$$\lambda_1(z) = c_1^2 z^2 \tanh\left(\frac{c_2^4 z^2}{c_1^2}\right), \quad (3)$$

where  $c_1$  and  $c_2$  are free parameters. This model can not only capture the confinement characteristics of QCD, but also simulate gluon condensation.

Although these two models have seen many successful applications [23, 26, 30, 40, 41], the study of pion meson structure remains insufficient—specifically, they cannot simultaneously describe multiple observables characterizing its internal structure. This indicates that these models fail to successfully capture the dynamics of pion mesons.

Inspired by Reference [14], we model QCD by modifying the  $AdS_5$  metric rather than introducing the dilaton field as a prefactor to the action in this study. The key properties of non-perturbative QCD are encoded by this modified background geometry. We assume the form of the modified metric to be

$$ds^2 = \frac{e^{2k_1^2 z^2 (1 - k_2 \tanh(k_1^2 z^2))}}{z^2} (\eta_{\mu\nu} dx^\mu dx^\nu + dz^2) \quad (4)$$

$$= e^{2A(z)} (\eta_{\mu\nu} dx^\mu dx^\nu + dz^2),$$

where  $k_1$  and  $k_2$  are free parameters. The form of wrap factor  $A(z)$  is

$$A(z) = -\ln(z) + \alpha(z), \quad \alpha(z) = k_1^2 z^2 (1 - k_2 \tanh(k_1^2 z^2)). \quad (5)$$

In this formulation, the  $\alpha(z)$  field behaves at the UV boundary as follows:

$$\alpha(z) = k_1^2 z^2 - k_2 k_1^4 z^4. \quad (6)$$

According to the holographic dictionary, the  $z^4$  term maps to the dimension-4 gauge-invariant gluon condensate on the boundary. At the infrared (IR) boundary, it takes the following form:

$$\alpha(z) = k_1^2 z^2 - k_2 k_1^2 z^2. \quad (7)$$

This indicates that the term which holographically encodes the gluon condensate in the UV evolves into a quadratic form in the IR and thereby contributes to the IR dynamics.

This model incorporates the physical aspects of both forms described above. We first employ this model to calculate the mass spectrum of the pion, from which the model parameters can then be determined.

The five-dimensional action for the pion is [23, 26, 30, 42, 43]

$$S_\pi = \int d^4x dz \sqrt{-g} [g^{mn} \partial_m \Phi^* \partial_n \Phi - m_5^2 \Phi^* \Phi], \quad (8)$$

where  $\Phi$  represents the field of the pion and  $m_5$  is the five dimensional mass of pion. From action (8), one derives the following equations of motion:

$$\partial_m [\sqrt{-g} g^{mn} \partial_n \Phi] - \sqrt{-g} m_5^2 \Phi = 0, \quad (9)$$

where  $g^{mn} = e^{-2A(z)} \eta^{mn}$ . Eq. (9) can be written as:

$$\partial_m [e^{3A(z)} \eta^{mn} \partial_n \Phi] - e^{5A(z)} m_5^2 \Phi = 0. \quad (10)$$

Defining  $\omega(z) = -3A(z)$ , one can obtain

$$\partial_m [e^{-\omega(z)} \eta^{mn} \partial_n \Phi] - e^{\frac{-5\omega(z)}{3}} m_5^2 \Phi = 0. \quad (11)$$

Proceeding, we employ a plane wave ansatz. The amplitude is taken to have dependence only on the holographic coordinate  $z$ , while propagating in the transverse space  $x^\mu$  with momentum  $P^\mu$ .

$$\Phi(x^\mu, z) = \psi(z) e^{iP_\mu x^\mu}, \quad (12)$$

where  $P^2 = P^\mu P_\mu = -M_n^2$ . A Schrödinger-like equation is obtained after algebraic manipulation and the identification  $\psi(z) = e^{\frac{\omega(z)}{2}} \varphi(z)$ . The resulting equation is:

$$-\varphi''(z) + \left[ \frac{\omega'(z)^2}{4} - \frac{\omega''(z)}{2} + e^{\frac{-2\omega(z)}{3}} m_5^2 \right] \varphi(z) = M_n^2 \varphi(z). \quad (13)$$

Here,  $M_n$  represents the mass spectrum of the pion in four-dimensional spacetime, where the quantum number  $n = 1$  corresponds to the ground state, and  $n = 2, 3, \dots$  denote the excited states.

By solving Equation (13) with the parameter choice  $k_1 = 0.255, k_2 = 2.22, m_5^2 = -4.095$ , we obtain the pion mass spectrum. The 5D pion mass in this study deviates slightly from  $m_5^2 = -4$  predicted by light-front holographic mapping for a pseudoscalar field with  $J = L = 0$

$m_\pi$	n=1	n=2	n=3	n=4	n=5
PDG(MeV)	139.6	1300±100	1812±12	2070±35	
Our(MeV)	139.6	1406	1892	2066	2278
Model 1(MeV)	140	1019	1793		
Model 2(MeV)	140	1520	2120		

TABLE I. Comparison of the pion resonance mass spectrum between experimental values [44], other models [45, 46], and our calculations (Our)

[26]. The slight deviation naturally reflects the finite quark mass and higher-order contributions, which explicitly break conformal symmetry and effectively shift the 5D mass. Thus, this 5D mass should be understood as an effective mass parameter.

As summarized in Table I, our calculated mass spectrum for the pion is in reasonable agreement with the experimental data, albeit with some minor deviations. Compared to other studies in the literature, our results show improved accuracy. Consequently, the gravitational background we use provides a closer approximation to real QCD. In the following, we will employ the same set of parameters to compute other observables, thereby further assessing the effectiveness of our model.

### III. ELECTROMAGNETIC FORM FACTORS

As fundamental hadronic observables, form factors encode essential information about hadron structure and dynamics. They capture the critical interplay between perturbative and nonperturbative regimes, a proper description of which should facilitate the study of the transition from high- $Q^2$  (perturbative) to low- $Q^2$  (non-perturbative) dynamics.

In the holographic dual, the electromagnetic form factor is mapped to the coupling between an external EM field  $\phi^m(x^\mu, z)$  and a hadron bulk mode  $\Phi_P(x^\mu, z)$  in AdS space, as expressed in the following correspondence [26]:

$$\int d^4x dz \sqrt{-g} \Phi_{P'}^*(x^\mu, z) \overleftrightarrow{\partial}_m \Phi_P(x^\mu, z) \phi^m(x^\mu, z) \quad (14)$$

$$\sim (2\pi)^4 \delta^4(P' - P - q) \epsilon_\mu (P^\mu + P'^\mu) F(q^2),$$

where  $P$  and  $P'$  are the four-momenta of the initial and final pions, respectively, and  $q = P' - P$  is the four-momentum of the virtual photon, with  $q^2 = -Q^2$ . The polarization vector of the photon is denoted by  $\epsilon_\mu$ , and  $F(q^2)$  represents the electromagnetic form factor. Here,  $\Phi^* \overleftrightarrow{\partial}_m \Phi = \Phi^* (\partial_m \Phi) - (\partial_m \Phi^*) \Phi$ . The lower expression corresponds to the pion EMFF in physical spacetime. It is equivalent to a local coupling with the quark current  $J^\mu = \sum e_q \bar{q} \gamma^\mu q$ .

The action for the electromagnetic field is

$$S_\gamma = -\frac{1}{4} \int d^4x dz \sqrt{-g} F^{mn} F_{mn}, \quad (15)$$

where  $F_{mn} = \partial_m \phi_n - \partial_n \phi_m$  represents the electromagnetic field strength tensor. The equation of motion cor-

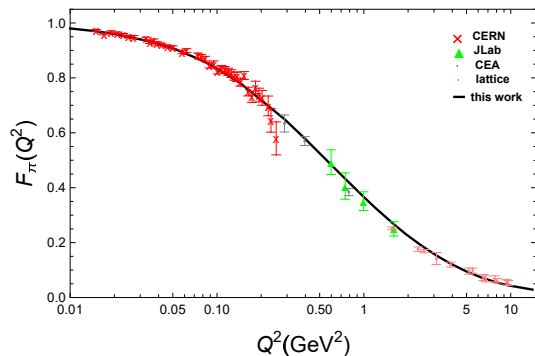


FIG. 1. The pion electromagnetic form factor  $F_\pi(Q^2)$ . The solid black line is our result, the pink points denotes lattice QCD data [47], and the other symbols represent experimental data [48–50].

responding to this action is

$$\partial_m [\sqrt{-g} F^{mn}] = 0. \quad (16)$$

The gauge condition is

$$\partial_\mu \phi_\mu + e^{-A(z)} \partial_z (e^{-A(z)} \phi_z) = 0. \quad (17)$$

We analyze the propagation of an electromagnetic probe (polarized along the Minkowski coordinates) through AdS spacetime,

$$\phi_\mu(x, z) = \epsilon_\mu e^{iq_\mu x^\mu} V(Q^2, z), \quad \phi_z = 0. \quad (18)$$

Its equation of motion is

$$[\partial_z^2 + A'(z) \partial_z - Q^2] V(Q^2, z) = 0. \quad (19)$$

The corresponding boundary conditions are

$$V(Q^2, 0) = V(0, z) = 1. \quad (20)$$

Then, the electromagnetic form factor of the pion can be written as

$$F_\pi(Q^2) = \int dz e^{3A(z)} \psi(z) V(Q^2, z) \psi(z). \quad (21)$$

The charge radius, a key observable for probing internal hadron structure, quantifies the spatial extent of the electric charge distribution.

Our analysis is performed in the Breit frame. The relevant kinematic variables— $\Delta^\nu, P^\nu$ , and the squared momentum transfer are given by [51]:

$$P^\nu = (E, \vec{0}), \quad \Delta^\nu = (0, \vec{\Delta}), \quad \Delta^2 = -Q^2, \quad (22)$$

where  $\Delta^\nu = P'^\nu - P^\nu$ . The spatial distribution of the form factor can be obtained via a Fourier transform:

$$F_\pi(r) = \int \frac{d^3\Delta}{(2\pi)^3} e^{-i\Delta \cdot \mathbf{r}} F_\pi(Q^2). \quad (23)$$

For the pion, the charge radius is given by:

$$\langle r_\pi^2 \rangle = \frac{\int d^3\mathbf{r} r^2 F_\pi(r)}{\int d^3\mathbf{r} F_\pi(r)} = -6 \frac{dF_\pi(Q^2)}{dQ^2} \Big|_{Q^2=0}. \quad (24)$$

	QCDSF	ETMC	Brandt	PDG	Our
$r_\pi(\text{fm})$	0.665	0.675	0.694	0.672	0.695

TABLE II. The pion charge radius. The first three data points are from lattice QCD [52–54], the fourth is the experimental value [44], and the last one is our result.

Figure 1 shows the  $Q^2$  dependence of the pion electromagnetic form factor. Our calculation is in good agreement with experimental and lattice QCD data. A chi-square test yields  $\chi^2/dof \approx 0.85$  for 42 data points, indicating that the deviation between the model and the data is comparable to the experimental uncertainties. Furthermore, the extracted charge radius of  $r_\pi = 0.695$  fm is consistent with lattice results and exhibits a mere 3.4% relative deviation from experiment (see Table II). These results suggest that our model captures the main electromagnetic properties of the pion to a reasonable extent.

#### IV. GRAVITATIONAL FORM FACTORS

GFFs provide the indispensable framework for exploring hadrons' generalized matter distributions (energy, momentum, pressure) at femtoscale. In the pion—a Nambu-Goldstone boson—these GFFs embed both the basic mass structure generated by dynamical chiral symmetry breaking and the internal mechanical traits that underlie its stability. Thus, computing the pion's GFFs precisely is essential for a first-principles understanding of how mass and spatial structure emerge in QCD. Building on the holographic QCD model constructed previously, this chapter focuses on computing the gravitational form factor  $A$  of the pion. Within the holographic duality framework, this form factor corresponds to the coupling between the tensor graviton fluctuation and the scalar field (dual to the pion) in AdS space.

The energy-momentum tensor of the pion can be written as [30]

$$T^{\mu\nu}(x, z) = \frac{-2}{\sqrt{-g}} \frac{\delta S_\pi}{\delta g_{\mu\nu}}. \quad (25)$$

Plugging the metric perturbation into the action gives the interaction action that couples the graviton to the pion field.

$$S_{int} = \frac{1}{2} \int d^4x dz \sqrt{-g} h_{\mu\nu} T^{\mu\nu} + o(h^2). \quad (26)$$

The graviton's equation of motion is obtained from the gravitational action  $S_G$  by inserting the metric perturbation  $\eta'_{\mu\nu} = \eta_{\mu\nu} + h_{\mu\nu}$ . We can get

$$S_h = \frac{1}{4\kappa^2} \int d^4x dz \sqrt{-g} (\partial_\lambda h^{\mu\nu} \partial^\lambda h_{\mu\nu} - \frac{1}{2} \partial_\lambda h \partial^\lambda h), \quad (27)$$

where  $h$  represent the trace  $h^\mu_\mu$  and  $\kappa$  is the Newton constant. By imposing the harmonic-traceless gauge

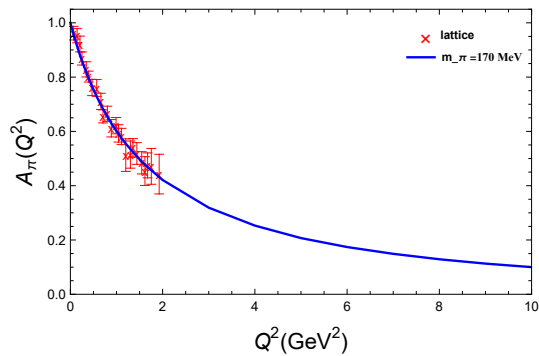


FIG. 2. The pion gravitational form factor  $A_\pi(Q^2)$ . The solid blue line is our result, and the red crosses represent lattice results [55].

$\partial_\lambda h_n^\lambda = \partial_n h = 0$ , we arrive at the graviton's equation of motion:

$$[\partial_z^2 + 3A'(z)\partial_z - Q^2]H(Q^2, z) = 0, \quad (28)$$

where  $h_{\mu\nu} = \epsilon_{\mu\nu} e^{-iq_G x} H(Q^2, z)$ ,  $q_G^2 = -Q^2$ . The corresponding boundary conditions are:

$$H(Q^2, 0) = H(0, z) = 1, \quad \partial_z H(Q^2, \infty) = 0. \quad (29)$$

The matrix element of the energy-momentum tensor for the pion can be expressed as [32]

$$\langle P' | T_{\mu\nu} | P \rangle = 2P_\mu P_\nu A_\pi(Q^2) + \frac{1}{2} (\Delta_\mu \Delta_\nu - \eta_{\mu\nu} \Delta^2) D_\pi(Q^2), \quad (30)$$

where GFFs  $A_\pi(Q^2)$  and  $D_\pi(Q^2)$  are related to the internal momentum and pressure distributions inside the pion. In this chapter, we restrict our calculation to the GFF  $A_\pi(Q^2)$ .

We then obtain the gravitational form factor of the pion:

$$A_\pi(Q^2) = \int dz e^{3A(z)} \psi(z) H(Q^2, z) \psi(z). \quad (31)$$

As shown in Figure 2, the red crosses denote the lattice QCD results for a pion mass of 170 MeV, while the blue solid line represents our result at the corresponding pion mass. We can see that our result is in basic agreement with the lattice calculation.

Our model simultaneously describes the pion mass spectrum, electromagnetic form factors, and gravitational form factors, yielding results in agreement with both experimental measurements and lattice QCD calculations. This suggests the potential usefulness of our model. In the next chapter, we will extend our calculation to the form factors of pion excited states and investigate the dependence of the pion form factors on its mass.

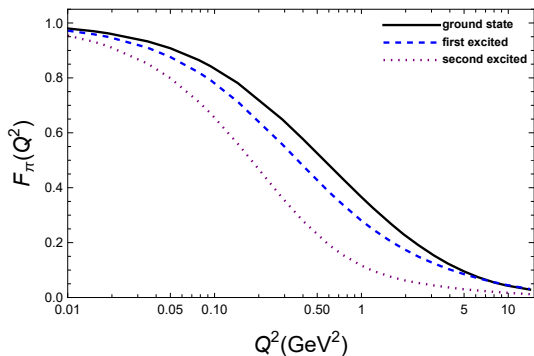


FIG. 3. The pion electromagnetic form factor  $F_\pi(Q^2)$  for different states. The black line, dashed line and dotted line represent the ground state, the first excited state and the second excited state of pion respectively.

### V. EMFF AND GFF OF PION EXCITED STATES AND THEIR PION-MASS DEPENDENCE

Although the formal expressions for the electromagnetic and gravitational form factors are identical for both ground and excited states—stemming from the same underlying symmetry currents—their physical content differs significantly. While the ground-state pion is well constrained by experiment and serves as a benchmark for model validation, its radial or orbital excitations probe the internal structure of QCD bound states in regimes dominated by higher Fock components, stronger relativistic effects, or altered chiral dynamics. Moreover, investigating the pion’s excited states within our framework not only tests the model’s predictive power beyond the ground state but also provides insights into how hadronic structure evolves with excitation energy and quark mass.

In the following, we present results for the electromagnetic and gravitational form factors of the excited state of the pion, computed using the same formalism as in the ground-state case (see Sections II and III), with the only modification being the replacement of the pion ground-state field by the excited-state field, as obtained from Eq. (13). The corresponding numerical results are shown in Figs. 3 and 4.

Both the EMFF  $F_\pi(Q^2)$  and the GFF  $A_\pi(Q^2)$  of the pion satisfy the normalization condition  $F_\pi(0) = A_\pi(0) = 1$  for ground and excited states alike, reflecting charge conservation and energy-momentum conservation, respectively. Remarkably, the excited-state form factors exhibit a universal qualitative behavior: they fall off more rapidly with increasing momentum transfer  $Q^2$  compared to their ground-state counterparts. This means that the excited-state form factor has a larger slope, corresponding to a larger radius, signaling a more spatially extended internal structure—whether in terms of charge or energy-momentum distribution. This spatial diffuseness can be traced back to a weaker effective interaction among the constituent quarks inside the excited state, which in

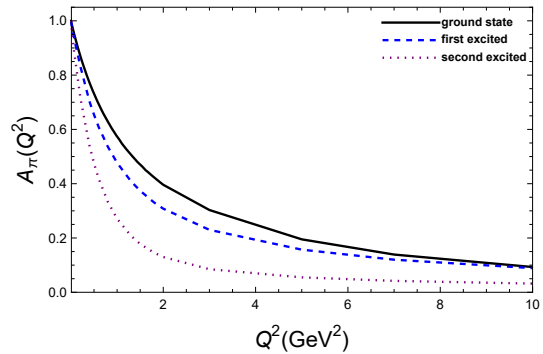


FIG. 4. The pion gravitational form factor  $A_\pi(Q^2)$  for different states. The black line, dashed line and dotted line represent the ground state, the first excited state and the second excited state of pion respectively.

momentum space suppresses the high-momentum tail. Despite these differences at low and intermediate  $Q^2$ ,  $F_\pi(Q^2)$  converges toward the same asymptotic behavior at large  $Q^2$ . This suggests that, in the deep space-like regime where short-distance quark-gluon dynamics dominate, the memory of radial excitation is effectively washed out, and the form factors are governed by universal perturbative QCD scaling laws. Furthermore, the faster flattening of the excited-state form factors indicates that they enter the perturbative QCD regime more quickly. These features are clearly illustrated in Figures 3 and 4.

To further investigate the robustness of our model and to explore the dependence of form factors on the pion mass, we extend our analysis to different values of  $m_\pi$ . Through varying the metric parameter  $k_1$ , we obtain the ground-state wave functions corresponding to different pion masses by solving Eq. (13). Substituting these wave functions into the formulas then allows us to compute the electromagnetic and gravitational form factors, thereby probing how variations in quark masses affect the internal structure of hadrons. We have calculated the ground-state electromagnetic and gravitational form factors for  $m = 0$  MeV, 140 MeV, and 300 MeV, respectively, as shown in Figures 5 and 6. This is also relevant for understanding the chiral dynamics within QCD and for checking theoretical models across a somewhat wider range of parameters.

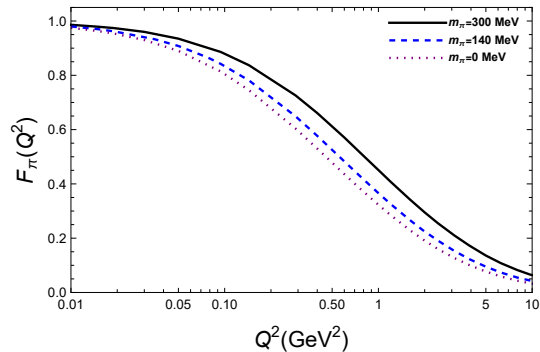


FIG. 5. The pion electromagnetic form factor  $F_\pi(Q^2)$  for different mass. The black line, dashed line and dotted line represent  $m_\pi = 300$  MeV,  $m_\pi = 140$  MeV and  $m_\pi = 0$  MeV respectively.

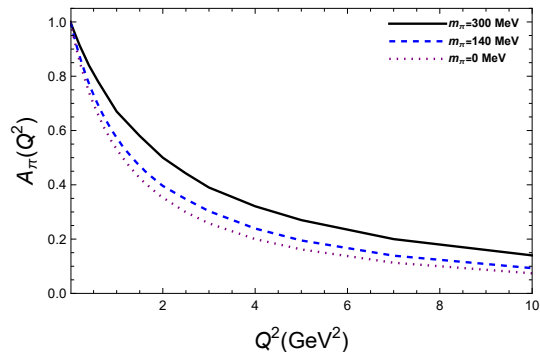


FIG. 6. The pion gravitational form factor  $A_\pi(Q^2)$  for different mass. The black line, dashed line and dotted line represent  $m_\pi = 300$  MeV,  $m_\pi = 140$  MeV and  $m_\pi = 0$  MeV respectively.

Both the EMFF  $F_\pi(Q^2)$  and the GFF  $A_\pi(Q^2)$  of the pion satisfy the normalization condition  $F_\pi(0) = A_\pi(0) = 1$  for all pion masses considered, as required by charge and energy-momentum conservation. However, at finite momentum transfer  $Q^2 > 0$ , we observe a systematic trend: the lighter the pion, the smaller the value of the form factors. This behavior is clearly displayed in Figures 5 and 6. The faster falloff of  $F_\pi(Q^2)$  and  $A_\pi(Q^2)$  with decreasing pion mass implies a larger slope at  $Q^2 = 0$ , which corresponds to a larger root-mean-square radius, thereby signaling a more spatially extended charge and energy-momentum distribution in lighter pions—consistent with the chiral dynamics expectation that the pion becomes increasingly diffuse and extended as  $m_\pi \rightarrow 0$ .

## VI. CONCLUSION

We introduce a phenomenologically deformed holographic model that incorporates key aspects of QCD—such as linear confinement and gluon condensation—and employed it to study the internal structure of the pion. In contrast to the conventional soft wall model, we break conformal invariance by modifying the warp factor of the  $AdS_5$  metric. This model includes a term that provides an effective description of the gluon condensate in the high-energy region, which evolves into a quadratic term that also contributes to the infrared dynamics, thus enabling us to better describe the confinement and other QCD properties of the pion.

This work simultaneously calculates the pion mass spectrum, electromagnetic form factors, charge radius, and gravitational form factors, all of which show reasonable agreement with experimental data and lattice QCD results. Subsequently, we extend the study to investigate the form factors of pion excited states and the mass dependence of these form factors. Together, these results suggest that the model provides a viable description.

A limitation of our model is that the modified warp factor is introduced phenomenologically, not derived dynamically. However, this phenomenological choice is reasonable and useful: despite being manually inserted, it captures key QCD features including confinement and gluon condensation. More importantly, its utility is supported by results—the model simultaneously describes multiple pion observables (mass spectrum, form factors, charge radius) in agreement with experiment and lattice QCD, and extends to excited states. Thus, the hand-built warp factor serves as a practical tool for studying the pion's internal structure.

To conclude, this study shows that a holographic model incorporating key QCD characteristics can consistently describe a range of pion observables. While some discrepancies remain, the model offers a useful platform for future research on non-perturbative strong interaction physics.

## ACKNOWLEDGMENTS

We thank Hai-cang Ren and Yan-Qing Zhao for useful discussions. This work is supported in part by the National Key Research and Development Program of China under Contract No. 2022YFA1604900. This work is also partly supported by the National Natural Science Foundation of China (NSFC) under Grants No. 12435009, and No. 12275104.

## REFERENCES

[1] T. Horn and C. D. Roberts, The pion: an enigma within the Standard Model, *J. Phys. G* **43**, 073001 (2016),

arXiv:1602.04016 [nucl-th].

- [2] A. C. Aguilar *et al.*, Pion and Kaon Structure at the Electron-Ion Collider, *Eur. Phys. J. A* **55**, 190 (2019), [arXiv:1907.08218 \[nucl-ex\]](#).
- [3] B. Ananthanarayan, Pions: the original Nambu–Goldstone bosons: An introduction and precision pion physics, *Eur. Phys. J. ST* **231**, 91 (2022).
- [4] R. J. Holt and C. D. Roberts, Distribution Functions of the Nucleon and Pion in the Valence Region, *Rev. Mod. Phys.* **82**, 2991 (2010), [arXiv:1002.4666 \[nucl-th\]](#).
- [5] J. M. Maldacena, The Large  $N$  limit of superconformal field theories and supergravity, *Adv. Theor. Math. Phys.* **2**, 231 (1998), [arXiv:hep-th/9711200](#).
- [6] E. Witten, Anti de Sitter space and holography, *Adv. Theor. Math. Phys.* **2**, 253 (1998), [arXiv:hep-th/9802150](#).
- [7] M. Natsuume, *AdS/CFT Duality User Guide*, Vol. 903 (2015) [arXiv:1409.3575 \[hep-th\]](#).
- [8] J. Polchinski and M. J. Strassler, Hard scattering and gauge / string duality, *Phys. Rev. Lett.* **88**, 031601 (2002), [arXiv:hep-th/0109174](#).
- [9] T. Gherghetta, J. I. Kapusta, and T. M. Kelley, Chiral symmetry breaking in the soft-wall AdS/QCD model, *Phys. Rev. D* **79**, 076003 (2009), [arXiv:0902.1998 \[hep-ph\]](#).
- [10] A. Karch, E. Katz, D. T. Son, and M. A. Stephanov, Linear confinement and AdS/QCD, *Phys. Rev. D* **74**, 015005 (2006), [arXiv:hep-ph/0602229](#).
- [11] E. Folco Capossoli, M. A. Martín Contreras, D. Li, A. Vega, and H. Boschi-Filho, Hadronic spectra from deformed AdS backgrounds, *Chin. Phys. C* **44**, 064104 (2020), [arXiv:1903.06269 \[hep-ph\]](#).
- [12] J. Deng and D. Hou, Nucleon structure from an AdS/QCD model in the Veneziano limit, *Phys. Rev. D* **112**, 036011 (2025), [arXiv:2502.00771 \[nucl-th\]](#).
- [13] X. Chen, Y. Chen, and K. Zhou, Data-driven Einstein-dilaton model for pure Yang-Mills thermodynamics and glueball spectrum, *Phys. Rev. D* **112**, 126025 (2025), [arXiv:2507.06729 \[hep-ph\]](#).
- [14] E. Folco Capossoli, M. A. Martín Contreras, D. Li, A. Vega, and H. Boschi-Filho, Proton structure functions from an AdS/QCD model with a deformed background, *Phys. Rev. D* **102**, 086004 (2020), [arXiv:2007.09283 \[hep-ph\]](#).
- [15] M. S. Tousi, K. Azizi, and H. R. Moshfegh, Investigation of the semileptonic decay  $\Xi_{cc}^{++} \rightarrow \Xi_c + \ell^+ \nu_\ell$  within QCD sum rules, *Phys. Rev. D* **110**, 114001 (2024), [arXiv:2409.00241 \[hep-ph\]](#).
- [16] T. M. Aliev, S. Bilmis, and M. Savci, Analysis of the light JP=3- mesons in QCD sum rules, *Phys. Rev. D* **108**, 034020 (2023), [arXiv:2307.00577 \[hep-ph\]](#).
- [17] G. F. de Teramond and S. J. Brodsky, Hadronic spectrum of a holographic dual of QCD, *Phys. Rev. Lett.* **94**, 201601 (2005), [arXiv:hep-th/0501022](#).
- [18] S. J. Brodsky and G. F. de Teramond, Hadronic spectra and light-front wavefunctions in holographic QCD, *Phys. Rev. Lett.* **96**, 201601 (2006), [arXiv:hep-ph/0602252](#).
- [19] C. Mondal, Longitudinal dynamics in light-front holographic QCD and hadron spectroscopy, *Rev. Mex. Fis. Suppl.* **3**, 0308091 (2022).
- [20] M. Ahmady, S. Kaur, C. Mondal, and R. Sandapen, Pion spectroscopy and dynamics using the holographic light-front Schrödinger equation and the 't Hooft equation, *Phys. Lett. B* **836**, 137628 (2023), [arXiv:2208.08405 \[hep-ph\]](#).
- [21] M. Ahmady and R. Sandapen, Predictions for pion and its excited states using light-front QCD holography and 't Hooft equation, *PoS ICHEP2024*, 540 (2025).
- [22] A. P. Bakulev, K. Passek-Kumericki, W. Schroers, and N. G. Stefanis, Pion form-factor in QCD: From nonlocal condensates to NLO analytic perturbation theory, *Phys. Rev. D* **70**, 033014 (2004), [Erratum: *Phys. Rev. D* **70**, 079906 (2004)], [arXiv:hep-ph/0405062](#).
- [23] S. J. Brodsky and G. F. de Teramond, Light-Front Dynamics and AdS/QCD Correspondence: The Pion Form Factor in the Space- and Time-Like Regions, *Phys. Rev. D* **77**, 056007 (2008), [arXiv:0707.3859 \[hep-ph\]](#).
- [24] H. J. Kwee and R. F. Lebed, Pion form-factors in holographic QCD, *JHEP* **01**, 027, [arXiv:0708.4054 \[hep-ph\]](#).
- [25] L. Chang, I. C. Cloët, C. D. Roberts, S. M. Schmidt, and P. C. Tandy, Pion electromagnetic form factor at space-like momenta, *Phys. Rev. Lett.* **111**, 141802 (2013), [arXiv:1307.0026 \[nucl-th\]](#).
- [26] S. J. Brodsky, G. F. de Teramond, H. G. Dosch, and J. Erlich, Light-Front Holographic QCD and Emerging Confinement, *Phys. Rept.* **584**, 1 (2015), [arXiv:1407.8131 \[hep-ph\]](#).
- [27] X. Gao, N. Karthik, S. Mukherjee, P. Petreczky, S. Syritsyn, and Y. Zhao, Pion form factor and charge radius from lattice QCD at the physical point, *Phys. Rev. D* **104**, 114515 (2021), [arXiv:2102.06047 \[hep-lat\]](#).
- [28] L.-B. Chen, W. Chen, F. Feng, and Y. Jia, Next-to-Next-to-Leading-Order QCD Corrections to Pion Electromagnetic Form Factors, *Phys. Rev. Lett.* **132**, 201901 (2024), [Erratum: *Phys. Rev. Lett.* **134**, 229901 (2025)], [arXiv:2312.17228 \[hep-ph\]](#).
- [29] S.-Q. Wang, Z.-F. Liao, J.-M. Shen, H. Zhou, J.-W. Zhang, J. Yan, X.-G. Wu, and L. Di Giustino, Analysis of the pion electromagnetic form factor with next-to-next-to-leading order QCD corrections, *Eur. Phys. J. C* **85**, 1435 (2025), [arXiv:2507.20479 \[hep-ph\]](#).
- [30] S. J. Brodsky and G. F. de Teramond, Light-Front Dynamics and AdS/QCD Correspondence: Gravitational Form Factors of Composite Hadrons, *Phys. Rev. D* **78**, 025032 (2008), [arXiv:0804.0452 \[hep-ph\]](#).
- [31] Y.-Z. Xu, M. Ding, K. Raya, C. D. Roberts, J. Rodríguez-Quintero, and S. M. Schmidt, Pion and kaon electromagnetic and gravitational form factors, *Eur. Phys. J. C* **84**, 191 (2024), [arXiv:2311.14832 \[hep-ph\]](#).
- [32] M. V. Polyakov and P. Schweitzer, Forces inside hadrons: pressure, surface tension, mechanical radius, and all that, *Int. J. Mod. Phys. A* **33**, 1830025 (2018), [arXiv:1805.06596 \[hep-ph\]](#).
- [33] W. Broniowski and E. Ruiz Arriola, Gravitational form factors of the pion and meson dominance, *Phys. Lett. B* **859**, 139138 (2024),

- arXiv:2405.07815 [hep-ph].
- [34] X.-H. Cao, F.-K. Guo, Q.-Z. Li, B.-W. Wu, and D.-L. Yao, Gravitational form factors of pions, kaons and nucleons from dispersion relations, *Eur. Phys. J. C* **82**, 626 (2022), arXiv:2204.09974 [hep-ph].
- [35] Y. Hatta and J. Schoenleber, Sullivan Process near Threshold and the Pion Gravitational Form Factors, *Phys. Rev. Lett.* **134**, 251901 (2025), arXiv:2502.12061 [hep-ph].
- [36] Y. Choi, H.-D. Son, and H.-M. Choi, Gravitational form factors of the pion in the self-consistent light-front quark model, *Phys. Rev. D* **112**, 014043 (2025), arXiv:2504.14997 [hep-ph].
- [37] K. K. Seth, S. Dobbs, Z. Metreveli, A. Tomaradze, T. Xiao, and G. Bonvicini, Electromagnetic Structure of the Proton, Pion, and Kaon by High-Precision Form Factor Measurements at Large Timelike Momentum Transfers, *Phys. Rev. Lett.* **110**, 022002 (2013), arXiv:1210.1596 [hep-ex].
- [38] D. Li and M. Huang, Dynamical holographic QCD model for glueball and light meson spectra, *JHEP* **11**, 088, arXiv:1303.6929 [hep-ph].
- [39] A. Vega and M. A. Martin Contreras, Melting of scalar hadrons in an AdS/QCD model modified by a thermal dilaton, *Nucl. Phys. B* **942**, 410 (2019), arXiv:1808.09096 [hep-ph].
- [40] A. Vega and M. A. Martin Contreras, Two-body light front wave functions from general AdS/QCD models, *Phys. Rev. D* **102**, 036017 (2020), arXiv:2005.04501 [hep-ph].
- [41] M. Á. Martín Contreras, A. Vega, and S. Cortés, Light pseudoscalar and axial spectroscopy using AdS/QCD modified soft wall model, *Chin. J. Phys.* **66**, 715 (2020), arXiv:1811.10731 [hep-ph].
- [42] G. F. de Teramond, H. G. Dosch, and S. J. Brodsky, Kinematical and Dynamical Aspects of Higher-Spin Bound-State Equations in Holographic QCD, *Phys. Rev. D* **87**, 075005 (2013), arXiv:1301.1651 [hep-ph].
- [43] H. G. Dosch, G. F. de Teramond, and S. J. Brodsky, Holographic light-front QCD, *J. Subatomic Part. Cosmol.* **5**, 100339 (2026), arXiv:2510.20180 [hep-ph].
- [44] R. L. Workman *et al.* (Particle Data Group), Review of Particle Physics, *PTEP* **2022**, 083C01 (2022).
- [45] M. Rinaldi, F. A. Ceccopieri, and V. Vento, The pion in the graviton soft-wall model: phenomenological applications, *Eur. Phys. J. C* **82**, 626 (2022), arXiv:2204.09974 [hep-ph].
- [46] Y. Li and J. P. Vary, Light-front holography with chiral symmetry breaking, *Phys. Lett. B* **825**, 136860 (2022), arXiv:2103.09993 [hep-ph].
- [47] H.-T. Ding, X. Gao, A. D. Hanlon, S. Mukherjee, P. Petreczky, Q. Shi, S. Syritsyn, R. Zhang, and Y. Zhao, QCD Predictions for Meson Electromagnetic Form Factors at High Momenta: Testing Factorization in Exclusive Processes, *Phys. Rev. Lett.* **133**, 181902 (2024), arXiv:2404.04412 [hep-lat].
- [48] S. R. Amendolia *et al.* (NA7), A Measurement of the Space - Like Pion Electromagnetic Form-Factor, *Nucl. Phys. B* **277**, 168 (1986).
- [49] C. L. Arnold, B. P. Roe, and D. Sinclair, Measurement of the form-factors in the decay  $k^+ \rightarrow \pi^+ \mu^+ \nu$ , *Phys. Rev. D* **9**, 1221 (1974).
- [50] J. Volmer *et al.* (Jefferson Lab F(pi)), Measurement of the Charged Pion Electromagnetic Form-Factor, *Phys. Rev. Lett.* **86**, 1713 (2001), arXiv:nucl-ex/0010009.
- [51] Z. Dehghan, F. Almaksusi, and K. Azizi, Mechanical properties of proton using flavor-decomposed gravitational form factors, *JHEP* **06**, 025, arXiv:2502.16689 [hep-ph].
- [52] D. Brömmel *et al.* (QCDSF/UKQCD), The Pion form-factor from lattice QCD with two dynamical flavours, *Eur. Phys. J. C* **51**, 335 (2007), arXiv:hep-lat/0608021.
- [53] R. Frezzotti, V. Lubicz, and S. Simula (ETM), Electromagnetic form factor of the pion from twisted-mass lattice QCD at  $N(f) = 2$ , *Phys. Rev. D* **79**, 074506 (2009), arXiv:0812.4042 [hep-lat].
- [54] B. B. Brandt, A. Jüttner, and H. Wittig, The pion vector form factor from lattice QCD and NNLO chiral perturbation theory, *JHEP* **11**, 034, arXiv:1306.2916 [hep-lat].
- [55] D. C. Hackett, P. R. Oare, D. A. Pefkou, and P. E. Shanahan, Gravitational form factors of the pion from lattice QCD, *Phys. Rev. D* **108**, 114504 (2023), arXiv:2307.11707 [hep-lat].